V International Conference on Computational Methods for Coupled Problems in Science and Engineering
COUPLED PROBLEMS 2013
S. Idelsohn, M. Papadrakakis and B. Schrefler (Eds)

MULTISCALE ANALYSIS OF PIEZOELECTRIC MATERIAL BY USING EBSD-MEASURED REALISTIC MODEL

HIROYUKI KURAMAE[*], HIDETOSHI SAKAMOTO[†] AND YASUTOMO UETSUJI[‡]

[*]Department of Technology Management, Faculty of Engineering
Osaka Institute of Technology
5-16-1 Omiya, Asahi-ku, Osaka 535-8585, Japan
e-mail: kuramae@dim.oit.ac.jp, www.oit.ac.jp

[†] Department of Mechanical System Engineering, Graduate School of Science and Technology
Kumamoto University
2-39-1 Kurokami, Kumamoto 860-8555, Japan
email: sakamoto@mech.kumamoto-u.ac.jp, www.kumamoto-u.ac.jp

[‡] Department of Mechanical Engineering, Faculty of Engineering
Osaka Institute of Technology
5-16-1 Omiya, Asahi-ku, Osaka 535-8585, Japan
email: uetsuji@med.oit.ac.jp, www.oit.ac.jp

Key words: Multiscale Analysis, Piezoelectric Material, RVE Modeling, ODF Analysis, Coupled Problem.

Abstract. Material properties of a polycrystal piezoelectric ceramic, a barium titanate $BaTiO_3$, were analyzed by the two-scale crystallographic homogenization method. Three-dimensional (3-D) micro-finite element (FE) model was constructed based on the electron backscatter diffraction (EBSD) measured crystal orientation distribution images. The images are piled up to a 3-D voxel data of crystal orientation distribution by repeating mechanically and chemically polishing, and EBSD measurement of the ceramic. We obtained 13 EBSD images of 128×100 pixels, which measurement interval was 0.635μm in-plane and the average amount of polishing was 1.66μm in thickness (normal) direction of specimen. Each voxel of EBSD was assigned into 8-node solid FE in-plane with maintaining resolution of EBSD measurement, and was divided into three FEs along thickness direction with same crystal orientation, because of improvement of aspect ratio of FE. The total number of FEs was 499,200 (=128×100×13×3) which corresponded to over two millions degrees of freedom. In order to realize a large-scale micro-analysis using EBSD-measured voxel FE model, the coupled problem of the piezoelectric material was solved by parallel conjugate gradient (CG) method combined with the block Gauss-Seidel (BGS) method. The coupled micro-FE equation to obtain characteristic function vectors was separated into two linear equations, such as the elastic deformation and electrostatic analyses, by employing the BGS method, and then the equations were solved by the parallel CG solver while substituting coupling terms each other. Therefore, nested iterative scheme was constructed on a PC cluster. In addition, the representative volume element (RVE) size was determined based on the orientation

distribution function analyses of EBSD voxel data. The least RVE size was 25,000μm^3, which corresponded to include 150 crystal grains.

1 INTRODUCTION

Piezoelectric ceramics, which have been used in actuators or sensors as a component of various electric and mechanical devices, consist of many crystal grains at a microscopic scale. Since each grain produces strongly anisotropic mechanical and electrical behaviour, the macroscopic properties of polycrystalline piezoelectric ceramics have large dependence of the microscopic crystal morphology. The multiscale analysis based on the homogenization method is needed for the piezoelectric materials to evaluate the effective macroscopic material properties [1]. Parallel processing technique is also required to the multiscale analysis because of large-scale coupling problem.

This paper presents a multiscale piezoelectric analysis based on the crystallographic homogenization method. In the finite element (FE) equation for the conventional piezoelectric analysis, coefficient matrix is not positive definite and strongly ill-condition because of coupling terms between mechanical and electrical fields [2-4]. In this study, a parallel computing technique for piezoelectric FE analysis is newly developed based on the iterative partitioned coupling method with the parallel conjugate gradient (CG) solver.

In order to construct a polycrystal microstructure model for the multi-scale FE analysis, a three-dimensional (3-D) representative volume element (RVE) which as crystal orientation distribution of a barium titanate ($BaTiO_3$) ceramic is measured by using the scanning electron microscope (SEM) with electron back scattered diffraction (EBSD) apparatus. Accuracy of solution is discussed through some numerical experiments. In addition, The optimum RVE size is determined based on the orientation distribution function (ODF) analysis of the EBSD-measured FE model.

2 METHOD OF THE ANALYSIS

2.1 Homogenization method for piezoelectric problem

A 3-D polycrystalline macro-continuum is formed by periodic microscopic structures of a RVE as shown in Fig. 1. The region Y of the RVE is made up of an aggregate of well-defined crystal grains and it is very small compared with the dimension of the overall macro-continuum region Ω, defined by a scale factor λ, which represents the reciprocal order of the repetition.

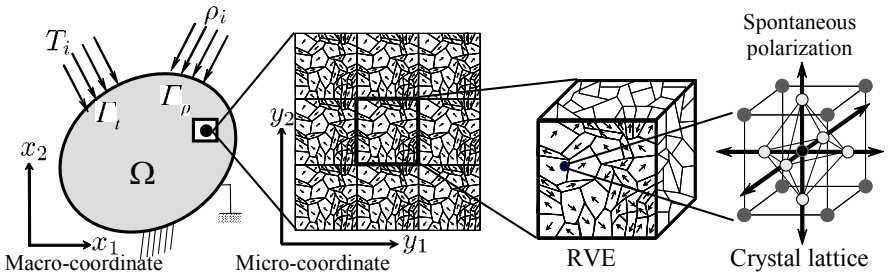

Figure 1: Macroscopic, microscopic and crystal structures for the multiscale finite element analysis based on the homogenization method

The piezoelectric elasticity constitutive equation for the Cauchy stress tensor σ_{ij} and the electric displacement vector D_i is expressed as follows:

$$\begin{aligned}\sigma_{ij} &= C^E_{ijkl}\varepsilon_{kl} - e_{kij}E_k \\ &= C^E_{ijkl}\frac{\partial u_k}{\partial x_l} + e_{kij}\frac{\partial \phi}{\partial x_k},\end{aligned} \tag{1}$$

$$\begin{aligned}D_i &= e_{ikl}\varepsilon_{kl} + \epsilon^S_{ik}E_k \\ &= e_{ikl}\frac{\partial u_k}{\partial x_l} - \epsilon^S_{ik}\frac{\partial \phi}{\partial x_k}.\end{aligned} \tag{2}$$

where the displacement vector u_k and the electric potential ϕ are selected as unknown variables in the piezoelectric problems, ε_{ij}, E_k are the strain tensor and the electric field, and $C^E_{ijkl}, e_{kij}, \epsilon^S_{ik}$ are the elastic compliance constant tensor, the piezoelectric strain constant, the dielectric constant tensor, respectively. The virtual work principle equation for the piezoelectric material is expressed as:

$$\int_{\Omega^\lambda}\left(C^{E\lambda}_{ijkl}\frac{\partial u_k}{\partial x_l} + e^\lambda_{nij}\frac{\partial \phi}{\partial x_n}\right)\frac{\partial \delta u_i}{\partial x_j}\mathrm{d}\Omega = \int_{\Gamma_t} t_i\delta u_i \mathrm{d}\Gamma, \tag{3}$$

$$\int_{\Omega^\lambda}\left(e^\lambda_{mkl}\frac{\partial u_k}{\partial x_l} - \epsilon^{S\lambda}_{mn}\frac{\partial \phi}{\partial x_n}\right)\frac{\partial \delta \phi}{\partial x_m}\mathrm{d}\Omega = \int_{\Gamma_\rho} \rho\delta\phi \mathrm{d}\Gamma. \tag{4}$$

In the homogenization procedure, macroscopic material properties C^{EH}_{ijmn}, e^H_{pij} and ϵ^{SH}_{ip} are obtained from the characteristic function by volume averaging in the RVE as follows:

$$C^{EH}_{ijmn} = \frac{1}{|Y|}\int_Y\left({}^{\mathrm{micro}}C^E_{ijmn} + {}^{\mathrm{micro}}C^E_{ijkl}\frac{\partial \chi^{mn}_k}{\partial y_l} + {}^{\mathrm{micro}}e_{kij}\frac{\partial \varphi^{mn}}{\partial y_k}\right)\mathrm{d}Y, \tag{5}$$

$$e^H_{pij} = \frac{1}{|Y|}\int_Y\left({}^{\mathrm{micro}}e_{pij} + {}^{\mathrm{micro}}e_{kij}\frac{\partial R^p}{\partial y_k} + {}^{\mathrm{micro}}C^E_{ijkl}\frac{\partial \Phi^p_k}{\partial y_l}\right)\mathrm{d}Y, \tag{6}$$

$$\epsilon^{SH}_{ip} = \frac{1}{|Y|}\int_Y\left({}^{\mathrm{micro}}\epsilon^S_{ip} + {}^{\mathrm{micro}}\epsilon^S_{ik}\frac{\partial R^p}{\partial y_k} - {}^{\mathrm{micro}}e_{ikl}\frac{\partial \Phi^p_k}{\partial y_l}\right)\mathrm{d}Y. \tag{7}$$

We assume that the piezoelectric material may have averaged properties in a macro continuum body. The characteristic function vectors $\{\boldsymbol{\chi}^{mn}\}$, $\{\boldsymbol{\varphi}^{mn}\}$, $\{\boldsymbol{\Phi}^p\}$ and $\{\boldsymbol{R}^p\}$ are obtained by solving the microscopic FE equations for the RVE as follows:

$$\begin{bmatrix}\mathbf{K}_{uu} & \mathbf{K}_{u\phi}\\ \mathbf{K}_{\phi u} & -\mathbf{K}_{\phi\phi}\end{bmatrix}\begin{Bmatrix}\boldsymbol{\chi}^{mn}\\ \boldsymbol{\varphi}^{mn}\end{Bmatrix} = \begin{Bmatrix}\boldsymbol{t}^{mn}\\ \boldsymbol{q}^{mn}\end{Bmatrix}, \quad (m,n) = (1,1),(2,2),(3,3),(1,2),(1,3),(2,3), \tag{8}$$

$$\begin{bmatrix}\mathbf{K}_{uu} & \mathbf{K}_{u\phi}\\ \mathbf{K}_{\phi u} & -\mathbf{K}_{\phi\phi}\end{bmatrix}\begin{Bmatrix}\boldsymbol{\Phi}^p\\ \boldsymbol{R}^p\end{Bmatrix} = \begin{Bmatrix}\boldsymbol{t}^p\\ \boldsymbol{q}^p\end{Bmatrix}, \quad p = 1,2,3, \tag{9}$$

where the characteristic functions have 9 components. The right-hand side vectors $\{\boldsymbol{t}^{mn}\}$, $\{\boldsymbol{q}^{mn}\}$, $\{\boldsymbol{t}^p\}$ and $\{\boldsymbol{q}^p\}$ are the constant values caused by the microscopic inhomogeneous structure. The coefficient matrices in both the linear equations are symmetric because of $[\mathbf{K}_{u\phi}] = [\mathbf{K}_{\phi u}]^T$. The size of the linear equation depends on the number of nodal points in the RVE FE model, and the degrees of freedom may be a large number for the EBSD-measured FE model.

Since the diagonal terms in the sub-matrix $[-\mathbf{K}_{\phi\phi}]$ are negative, the coefficient matrix of both the liner equations (8) and (9) is not positive definite. Since difference of numerical

order between $[\mathbf{K}_{uu}]$ and $[\mathbf{K}_{\phi\phi}]$ is very large more than 10^{24} in actual problem, the coefficient matrix is strongly ill-condition. Therefore, the iterative solver such as the CG method, which is well-suited for distributed memory type parallel computing environment such as a PC cluster, is inapplicable to the equations.

2.2 Iterative coupling method based on Block Gauss-Seidel method

In order to apply the CG method to solve the system equations, they are rewritten to a partitioned form based on the Block Gauss-Seidel (BGS) method as follow:

$$\begin{bmatrix} \mathbf{K}_{uu} & \mathbf{0} \\ -\mathbf{K}_{\phi u} & \mathbf{K}_{\phi\phi} \end{bmatrix} \begin{Bmatrix} \boldsymbol{u} \\ \boldsymbol{\phi} \end{Bmatrix}^{(k+1)} = \begin{Bmatrix} \boldsymbol{t} \\ -\boldsymbol{q} \end{Bmatrix} - \begin{bmatrix} \mathbf{0} & \mathbf{K}_{u\phi} \\ \mathbf{0} & \mathbf{0} \end{bmatrix} \begin{Bmatrix} \boldsymbol{u} \\ \boldsymbol{\phi} \end{Bmatrix}^{(k)} \tag{10}$$

where unknown vector $\{\boldsymbol{u}\}$ corresponds to $\{\boldsymbol{\chi}^{mn}\}$ and $\{\boldsymbol{\Phi}^{p}\}$, and $\{\boldsymbol{\phi}\}$ corresponds to $\{\boldsymbol{\varphi}^{mn}\}$ and $\{\boldsymbol{R}^{p}\}$, respectively. According the coupling term $[\mathbf{K}_{u\phi}]$ is moved to right hand side, displacement $\{\boldsymbol{u}\}$ and electrostatic potential $\{\boldsymbol{\phi}\}$ vectors are partitioned to maintain positive definite of both the coefficient matrices as follows:

$$[\mathbf{K}_{uu}]\{\boldsymbol{u}\}^{(k+1)} = \{\boldsymbol{t}\} - [\mathbf{K}_{u\phi}]\{\boldsymbol{\phi}\}^{(k)}, \tag{11}$$

$$[\mathbf{K}_{\phi\phi}]\{\boldsymbol{\phi}\}^{(k+1)} = -\{\boldsymbol{q}\} + [\mathbf{K}_{\phi u}]\{\boldsymbol{u}\}^{(k+1)}. \tag{12}$$

The parallel CG solver [5], which is parallelized on the inner product of the coefficient matrix and the descent direction vector by row block distribution of the coefficient matrix, is applied to each partitioned equation until unknown vectors $\{\boldsymbol{u}\}$ and $\{\boldsymbol{\phi}\}$ are converged with mutually substituting the coupling terms based on the BGS method as shown in Fig. 2. A nested iteration procedure of the BGS method including the CG iteration is constructed in this scheme.

In this study, a hierarchical process distribution technique is introduced to reduce amount of data for communication. The CPUs of PC cluster are logically divided into 9 processor groups, and allocated to the micro FE equations using the partitioning form. In each processor group, the parallel CG solver based on the block partitioning is applied to the linier equations. The parallel analysis code is implemented by using the Fortran 90 language and the message passing interface (MPI) library MPICH 1.2 [6].

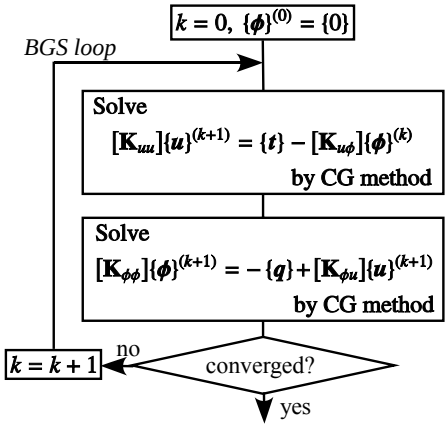

Figure 2: Flowchart of the iterative partitioned coupling procedure based on the block Gauss-Seidel (BGS) method

3 MULTISCALE ANALYSIS USING THREE-DIMENSIONAL EBSD-MEASURED MODEL

3.1 Three-dimensional EBSD measurement of barium titanate

We obtained distribution of crystal orientation in a 3-D parallelepiped box region of a $BaTiO_3$ ceramic (Murata Manufacturing Co. Ltd.) by using the EBSD (Oxford Instruments plc, Link ISIS C.7272) implemented in the SEM (JEOL Datum Ltd., JSM-5410) [5]. The specimen was a circular disk of 15mm diameter and 1mm thickness, and it was electrically poled along the thickness direction. The observed surface was mechanically polished using 3μm diamond particles (Marumoto Struers Co., DP-Spray) with a polishing sheet (DP-Mol). And then, it was chemically polished at pH3.5 using colloidal particles (OP-A) with a polishing sheet (DP-Chem). The surface of the isolative specimen was coated with the electrical conductive and amorphous osmium layer to defend the electrification due to electron beam. We employed an osmium coater (Meiwaforsis Co., Neoc-ST). In addition, a silver paste (Fujikura Kasei Co. Ltd., type D-500) was applied to the surface except for the SEM-EBSD measurement region to leak the accumulated charge.

Figure 3 shows crystal morphology images by the EBSD measurement. The scanning interval in plane direction was set to 0.635μm that is nearly smaller than one over ten of the average grain size. The interval of the polishing was set to 1.66μm in thickness direction. We obtained 13 images by repeating both the EBSD measurement and the polishing, and a 3-D EBSD model by the piled-up images as shown in Fig. 4. Therefore, the size of each voxel in the 3-D model is $0.635\times0.635\times1.660\mu m^3$. The average grain size was 6.71μm which was obtained by the intercept method.

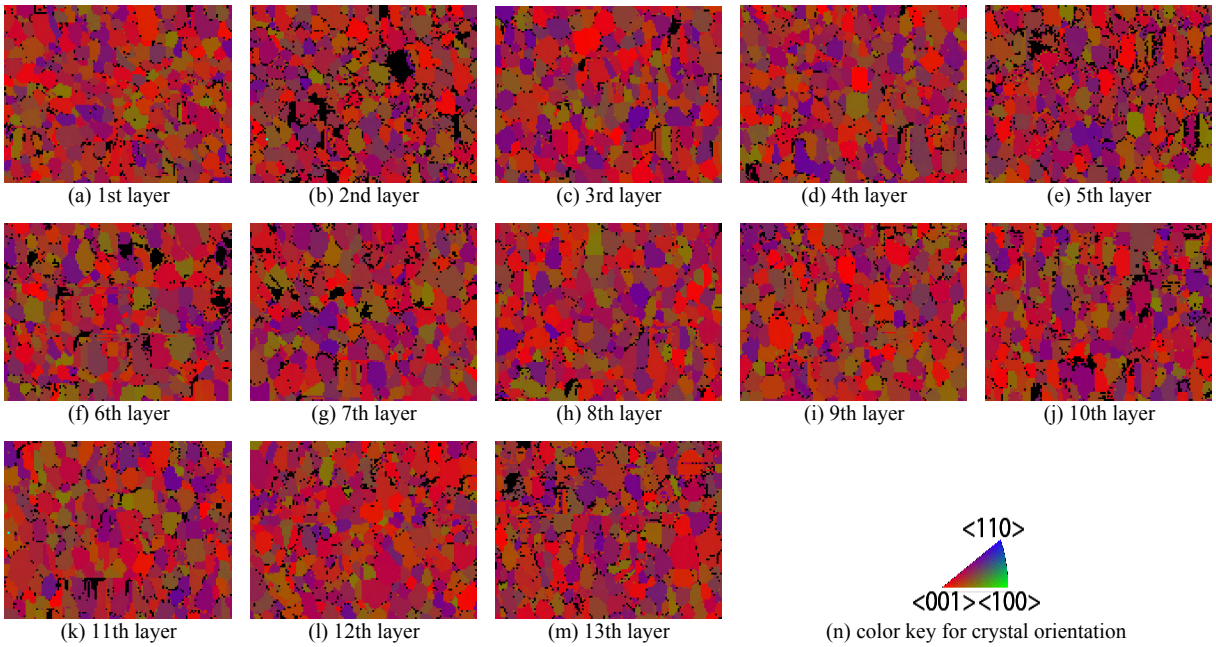

(a) 1st layer (b) 2nd layer (c) 3rd layer (d) 4th layer (e) 5th layer
(f) 6th layer (g) 7th layer (h) 8th layer (i) 9th layer (j) 10th layer
(k) 11th layer (l) 12th layer (m) 13th layer
(n) color key for crystal orientation

Figure 3: Crystal morphology images of a barium titanate (BaTiO3) ceramic by the SEM-EBSD measurement (measurement area: $81.3\times63.5\mu m^2$, number of measurement points: 128×100 pixels, interval of measurement: 0.635μm)

3.2 Three-dimensional modeling and results

A 3-D RVE FE model is constructed by using the EBSD measured images as shown in Fig. 4. The 13 layers of EBSD images are stacked into 3-D parallelepiped box. Using the 8-node isoparametric solid element, one crystal orientation image pixel is assigned to a FE in-plane, and each image layer is divided into three FEs in the thickness direction. The total finite elements are over 500 thousand in the 3D model as summerized in Tabel 1. It corresponds to over 2 million degrees of freedom in the micro finite equation.

In addition, two types of 2-dimensional (2-D) RVE FE models are also constructed to compare with the 3D model. One is the same in-plane size with the 3D model, which uses only the first layer of EBSD image, the other is employed for a large in-plane region, 2D-L model, which is constructed from four neighboring regions by EBSD measurements.

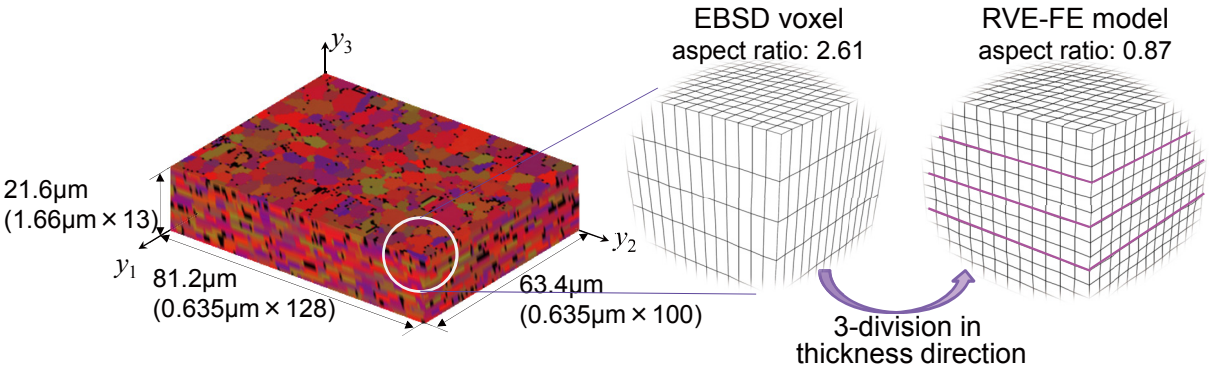

Figure 4: Three-dimensional RVE-FE modeling

Table 1: Properties of RVE-FE models

	Model size [μm] $y_1 \times y_2 \times y_3$	Number of finite elements	Number of nodes	Degrees of freedom	Element size [μm] $y_1 \times y_2 \times y_3$	Aspect ratio of element
2D model	63.5×81.3	100×128× 1= 12,800	20,058	104,232	0.635×0.635×0.635	1.00
2D-L model	90.8×90.8	143×143× 1= 20,449	41,472	165,888	0.635×0.635×0.635	1.00
3D model	63.5×81.3×21.6	100×128×39=521,160	521,160	2,084,640	0.635×0.635×0.553	0.87

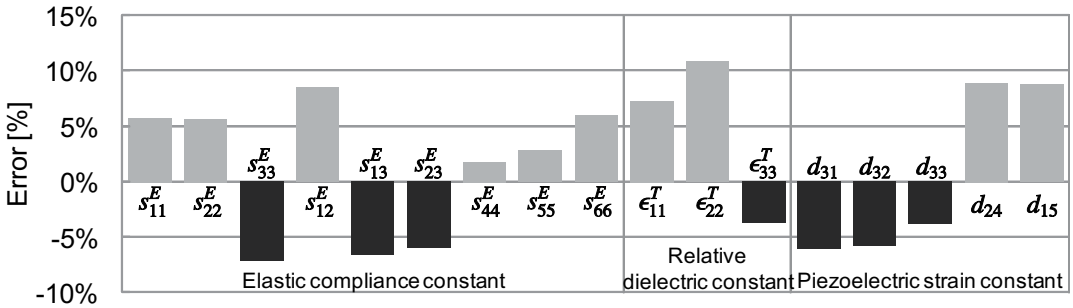

Figure 5: Complaison of accuracy of the homogenized material properties between 2D-L and 3D models

Figure 5 shows the homogenized material properties by using the 3-D RVE model compared with the 2D-L model. Comparing with the 2D-L model, the material properties of relation with thickness direction, such as s_{33}, s_{13} and s_{23}, are smaller than that of the 3D model

as shown in Fig. 5. In this study, Jaffe's experimental data [7] are used for single crystal material properties. In the 2-D analysis, since microscopic heterogeneity along thickness direction is excluded, material properties for in-plane are over estimated.

In order to investigate relation between the number of layers of 3-D RVE model and accuracy of the homogenized material properties, the employing number of EBSD image layers in 3-D model is changed. Figure 6 (a) shows relative error of homogenized material properties with the 3D model which has 13 EBSD image layers. The one layer case corresponds to 2D model. The errors are less than 5% in three layers or more sampling cases. Figure 6 (b) shows parallel analysis time using 36 cores of the AMD Opteron HE275 2.2GHz CPUs connected by the Giga-bit Ethernet (1Gbps) network. The parallel analysis time is linear by the number of FEs.

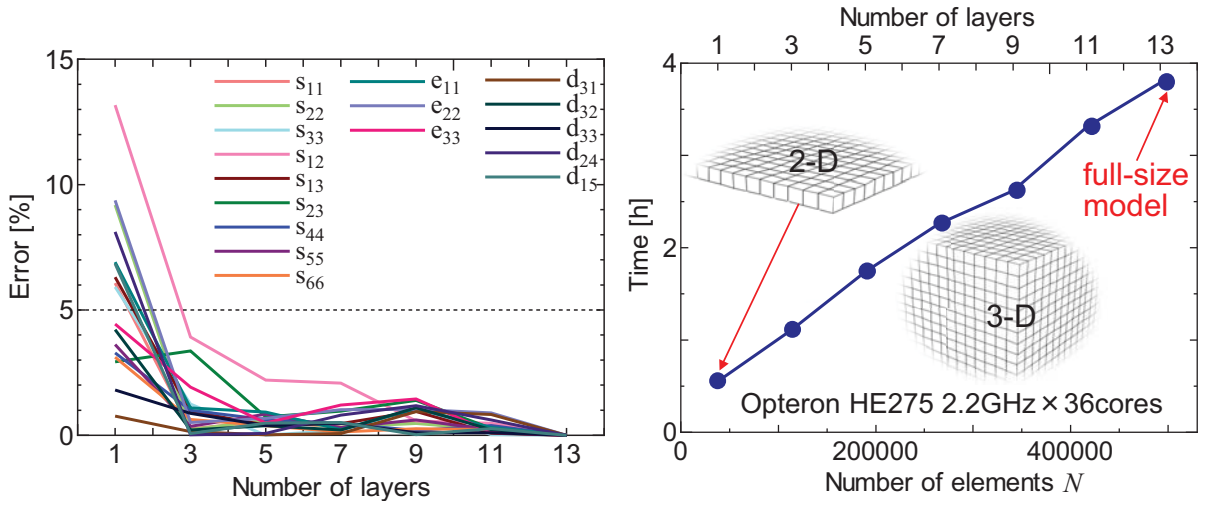

(a) Relationship between accuracy of homogenized material properties and number of sampling layers of the 3-D RVE-FE model

(b) Relationship between analysis time and number of elements (number of layers) of 3-D RVE-FE model

Figure 6: Relationship between number of sampling layers and accuracy, and analysis time

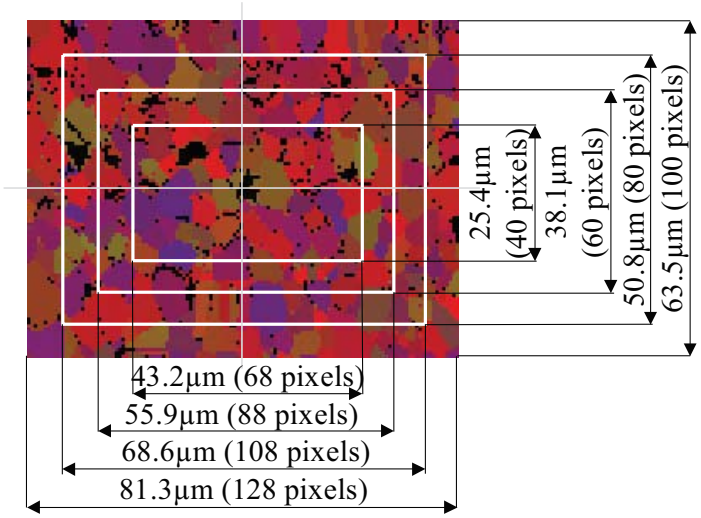

Figure 7: Image sampling of EBSD-measured crystal orientation distibution (4 types of plane size)

To investigate the optimum (minimum) RVE size, various sizes of RVE models were sampled from full-size EBSD model, in which 4 types of plane size as shown in Fig. 7, and 7 types of number of layers from center layer. The total 28 models are sampled as shown in Fig. 8. The one layer models as shown in Fig. 8 (a-1), (b-1), (c-1) and (d-1) are correspond to 2-D model, and 13 layers with 100×128 pixels as shown in Fig 8 (d-7) corredponds to the full-size 3D model.

Figure 9 shows relation between volume of models and the accuracy. The error bars in this figure means the smallest, the average and the largest errors of 17 components of the homogenized material properties. It is found that the accuracy is increased by the volume of RVE, and more than 25,000μm^3 volume of RVE is needed for less than 5% error of solution. The 25,000μm^3 volume of RVE contains 150 crystal grains due to average grain size 6.71μm.

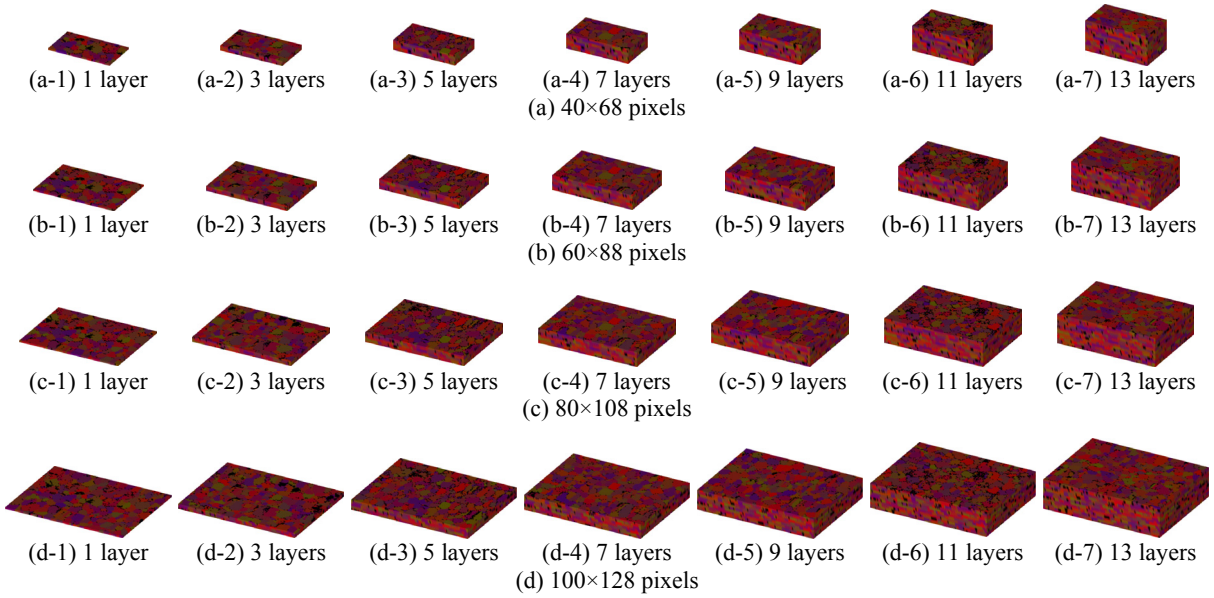

Figure 8: Sampling RVE models from full-size EBSD model (4 types of plane size and 7 types of number of layers)

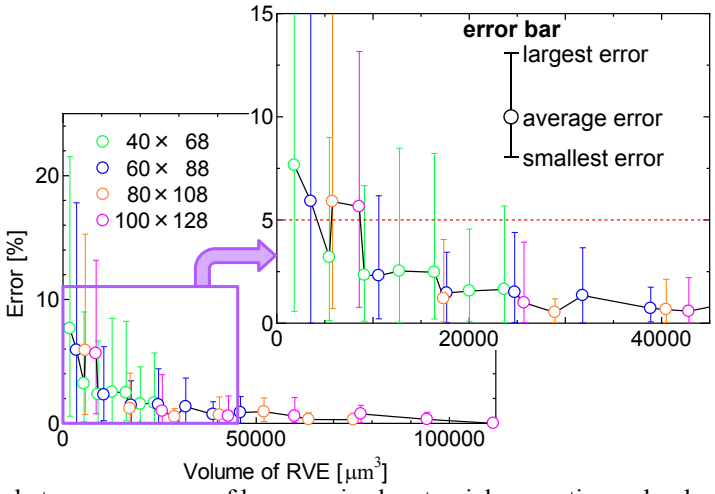

Figure 9: Relationship between accuracy of homogenized materuial properties and volume size of RVE model

4 RVE DETERMINATION BASED ON THE ODF ANALYSIS

To determine the optimum (minimum) RVE size, in this study, the orientation distribution function (ODF) analysis [8] is used. The ODF $f(\varphi_1, \Phi, \varphi_2)$ indicates intensity of the crystal orientation distribution in the Euler angle $(\varphi_1, \Phi, \varphi_2)$ space as follow:

$$f(\varphi_1, \Phi, \varphi_2) = \sum_{l=0}^{\infty} \sum_{m=-l}^{l} \sum_{n=-l}^{l} C_l^{mn} T_l^{mn}(\varphi_1, \Phi, \varphi_2), \tag{13}$$

where $T_l^{mn}(\varphi_1, \Phi, \varphi_2)$ and C_l^{mn} are spherical harmonic function and expansion coefficient, respectively. In this study, the ODF is analyzed for the crystal orientation distribution in RVE model every 5° in the Euler angle $(\varphi_1, \Phi, \varphi_2)$. Figure 10 shows results of the ODF intensity distribution in the 3-D Euler angle space for various sizes of RVE model. In the full-size 3D model which has 13 layers with 100×128 pixels as shown in Fig. 10 (d-7), some preferred orientations are appeared, but in the small model, the preferred orientation is disappeared. The larger model, the similar ODF distribution as full-size model is obtained. Therefore, the ODF results may be similar trend toward as accuracy of multiscale finite element results

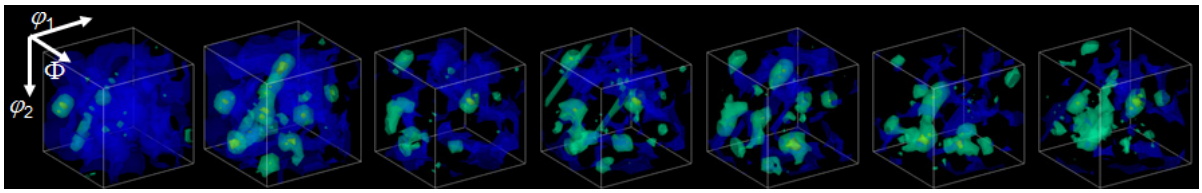

(a-1) 1 layer (a-2) 3 layers (a-3) 5 layers (a-4) 7 layers (a-5) 9 layers (a-6) 11 layers (a-7) 13 layers
(a) 40×68 pixels

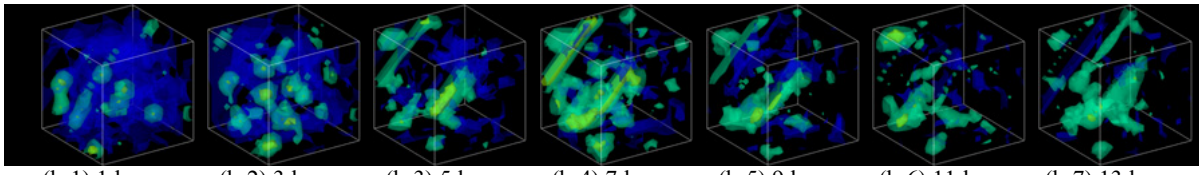

(b-1) 1 layer (b-2) 3 layers (b-3) 5 layers (b-4) 7 layers (b-5) 9 layers (b-6) 11 layers (b-7) 13 layers
(b) 60×88 pixels

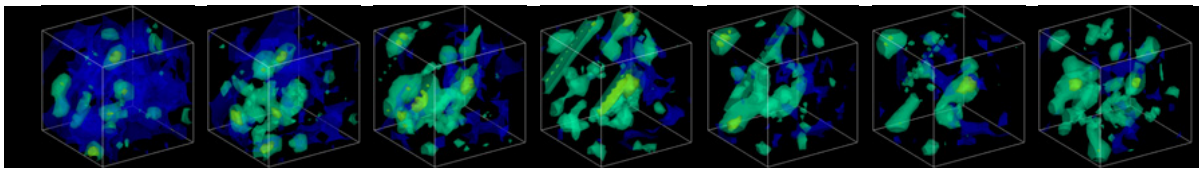

(c-1) 1 layer (c-2) 3 layers (c-3) 5 layers (c-4) 7 layers (c-5) 9 layers (c-6) 11 layers (c-7) 13 layers
(c) 80×108 pixels

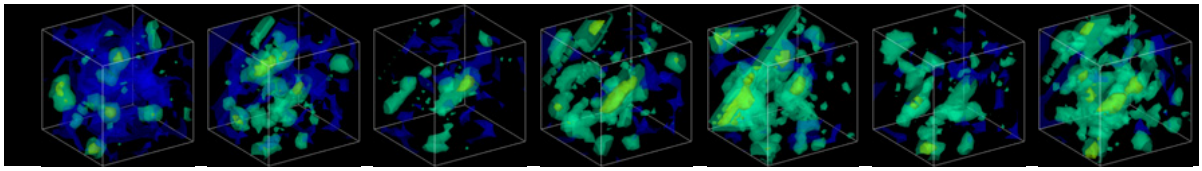

(d-1) 1 layer (d-2) 3 layers (d-3) 5 layers (d-4) 7 layers (d-5) 9 layers (d-6) 11 layers (d-7) 13 layers
(d) 100×128 pixels

Figure 10: ODF analysis results of various size of RVE models

In order to quantitively evaluate similarity of the ODF results between full-size model $f_{\text{full}}(\varphi_1, \Phi, \varphi_2)$ and sampled RVE model $f_{\text{sample}}(\varphi_1, \Phi, \varphi_2)$, error sum of square S of ODF intensity distribution in the Euler angle space every 5° is calculated as follow:

$$S = \frac{1}{N} \sum_{\varphi_1=0^\circ}^{90^\circ} \sum_{\Phi=0^\circ}^{90^\circ} \sum_{\varphi_2=0^\circ}^{90^\circ} \left[f_{\text{full}}(\varphi_1, \Phi, \varphi_2) - f_{\text{sample}}(\varphi_1, \Phi, \varphi_2) \right]^2, \tag{14}$$

where N is number of evaluation points in the Euler angle space $N = 19 \times 19 \times 19 = 6{,}859$.

Figure 11 (a) shows comparison between error of homogenized material properties, which is multiscale FE results, and error sum of square of the ODF analyses. Similar decrease curve lines are indicated in this figure. Figuer 11 (b) shows scatter diagram of error of homogenized properties and the error sum of squares of ODF. The coefficient of correlation is 0.85. It is reveal correlation between accuracy of FE result and ODF errors. Threfore, estimation of error of homogenized material properties based on ODF analysis is effective to determine RVE size.

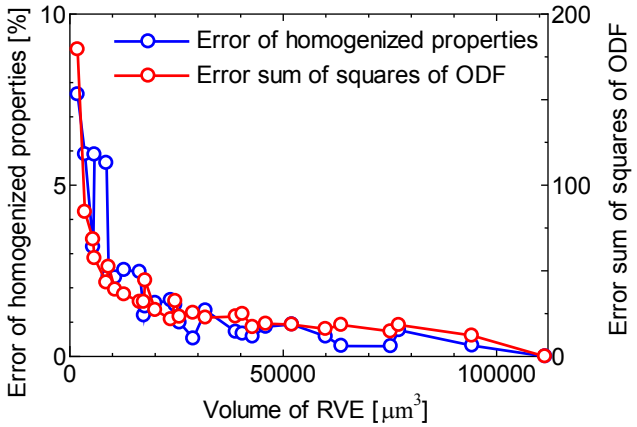

(a) Comparison between accuracy of multiscale FE results and error sum of squares of ODF

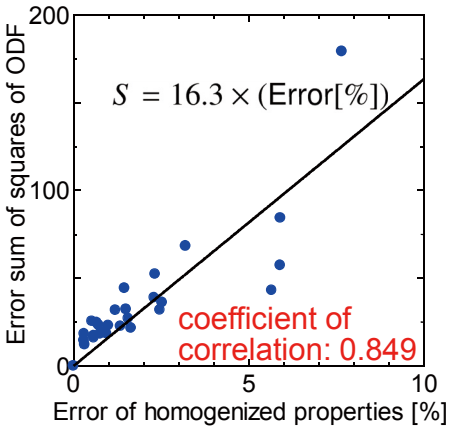

(b) Scatter diagram for correlation analysis between accuracy of multiscale FE results and error sum of squares of ODF

Figure 11: Determination of RVE size by ODF anarysis

5 CONCLUSIONS

3-D realistic RVE model based on the EBSD measurement images of crystal orientation distribution was constructed. Homogenized material properties by using several sizes of RVE models were obtained. Determination method of the optimum RVE size based on ODF analysis is proposed. In this time, over 25,000μm^3 volume size is required which contains 150 crystal grains due to average grain size.

REFERENCES

[1] Uetsuji, Y., Satou, Y., Nagakura, H., Nishioka, H., Kuramae, H. and Tsuchiya, K. Crystal morphology analysis of piezoelectric ceramics using electron backscatter diffraction method and its application to multiscale finite element analysis. *J. Comput. Sci. Tech.* (2008) **2**:568-577.

[2] Landis, C.M. A new finite-element formulation for electromechanical boundary value problems. *Int. J. Numer. Meth. Engng.* (2002) **55**:613-628.
[3] Asai, M., Takano, N., Uetsuji, Y. and Taki, K. An iterative solver applied to strongly coupled piezoelectric problems of porous $Pb(Zr,Ti)O_3$ with non-destructive modelling of microstructure. *Modelling Simul. Mater. Sci. Eng.* (2007) **15**:597-617.
[4] Kuramae, H. and Uetsuji Y. Parallel Iterative Partitioned Coupling Procedure for Multi-scale Piezoelectric Finite Element Analysis, *Proc. of 2nd International Conference on Computer Technology and Development*, (2010) 60-64.
[5] Horie, T. and Kuramae, H. Evaluation of parallel performance of large scale computing using workstation cluster. *Comput. Mech.* (1996) **17**:234-241.
[6] Pacheco, P. Parallel Programming with MPI. Morgan Kaufmann, (1996).
[7] Jaffe, B., Cook, W.R. and Jaffe, H. Piezoelectric ceramics. Academic Press London and New York, (1956).
[8] Bunge, H.J. *Texture Analysis in Material Science*. Butterworth, London, (1982).